Eur Phys J A (2004) **19**, s01, 71–76
Digital Object Identifier (DOI) 10.1140/epjad/s2004-03-012-2

EPJ A direct
electronic only

Baryon resonance analysis from two pion electroproduction at Jefferson Laboratory

Marco Ripani

INFN, Sezione di Genova, Via Dodecaneso 33, I-16146, Genova, Italy

Received: 31 July 2003 / Accepted: 14 Nov 2003 /
Published Online: 6 Feb 2004 –

Abstract. The cross section for the reaction $ep \to e'p\pi^+\pi^-$ was measured in the resonance region for 1.4<W<2.1 GeV and 0.5< Q^2 <1.5 GeV$^2/c^2$ using the CLAS detector at Jefferson Laboratory. The data show resonant structures not visible in previous experiments. The comparison of our data to a phenomenological prediction using available information on N^* and Δ states shows an evident discrepancy. A better description of the data is obtained either by a sizeable change of the properties of the $P_{13}(1720)$ resonance or by introducing a new baryon state, not reported in published analyses.

PACS. 13.60.Le Meson production – 13.40.Gp Electromagnetic form factors – 14.20.Gk Baryon resonances with S=0

1 Introduction

All existing information on baryon resonances has been obtained in experiments where a pion is present either in the incoming or in the outgoing channel ($\pi N \to \pi N$, $\gamma N \to \pi N$, etc.). It is therefore clear how these experiments are not suited to look for states with a weak pion coupling. Actually, many of the nucleon excited states in the mass region around and above 1.7 GeV tend to decouple from the single-pion and eta channels, while decaying predominantly in multipion channels, such as $\Delta\pi$ or $N\rho$[1]. A similar situation is expected for the "missing states"[2,3,4,5], predicted by symmetric quark models but lacking experimental evidence, whose search is carried on at several labs. Other models, with different symmetry properties and a reduced number of degrees of freedom, as e.g. in [6], predict fewer states. By using an electromagnetic probe to produce multipion final state, we have both the possibility of enhancing poorly known states in the mass region above 1.5 GeV, and of discovering new states. At the same time, the electromagnetic probe allows to study the transition form factors, that are predicted in quark models and whose knowledge is essential in understanding the degrees of freedom and the symmetries involved in the baryon wavefunctions[7,8]. It is therefore very important to extend our knowledge about the excited nucleon states by using the new powerful electron and photon beams in conjunction with multiparticle detection in the final state, to select different decay channels and explore their resonance content in much more detail than in the past. These capabilites are available at Jefferson Laboratory, where the high intensity and high quality continuous electron beam has been used in a variety of experiments aimed at a vast improvement of our understanding of the light quark baryon resonance properties[9], the so-called N* program. In this contribution, I will focus on a particular topic of this program , the measurement of baryon resonance properties in the double pion electroproduction channel, classified as JLab experiment E-93-006. In this experiment, the goal was to use electroproduction of pion pairs as a tool to investigate resonances of higher mass and achieve a better understanding of their properties, in particular the electromagnetic transition form factors, completely unknown for some states, and at the same time attempt to discover new states, predicted by quark models but still lacking experimental evidence. The cross sections measured with CLAS show clear resonant structures, not visible in the previous limited data, and calculations based on the known resonance properties or on quark model predictions are not able to fully account for the features observed, leading to a possible evidence for a contribution from a new state, not reported in the existing Particle Data Group (PDG) listing [1].

2 Generalities

Studying high-lying resonances involves new features and open issues. The presence of many broad, overlapping states makes it necessary to use appropriate filters to enhance particular states or a group of states. This is naturally accomplished using different decay channels to study selected states that manifest through a correspondingly large branching fraction. In particular, an important part of the CLAS experimental program at Jefferson Laboratory is devoted to the study of multipion channels, like

$\Delta\pi$ and ρN, with the goal of extracting information on the electromagnetic excitation of high-lying states weakly visible in single pion production, like the $D_{33}(1700)$, and of establishing the existence of the "missing" states predicted by the quark models.

In this talk I report on a measurement of the $ep \to e'p\pi^+\pi^-$ reaction studied with the CEBAF Large Acceptance Spectrometer (CLAS) at Jefferson Lab (JLab experiment E-93-006). More details on the experimental and physical analysis can be found in [10]. Beam currents of a few nA were delivered to Hall B on a liquid-hydrogen target, corresponding to luminosities up to 4×10^{33} cm^{-2}s^{-1}. Data were taken in 1999 for about two months at beam energies of 2.6 and 4.2 GeV. Important features of the CLAS [11] are its large kinematic coverage for multi-charged-particle final states and its good momentum resolution ($\Delta p/p \sim$1%). Using an inclusive electron trigger based on a coincidence between the forward electromagnetic shower calorimeter and the gas Cerenkov detector, many exclusive hadronic final states were measured simultaneously. Scattered electrons were identified through cuts on the calorimeter energy loss and the Cerenkov photo-electron distribution. Different channels were separated through particle identification using time-of-flight information and other kinematic cuts. We used the missing-mass technique, requiring detection in CLAS of at least $ep\pi^+$. The good resolution allowed selection of the exclusive final state, $ep\pi^+\pi^-$. After applying all cuts, our data sample included about 2×10^5 two-pion events.

The range of invariant hadronic center-of-mass (CM) energy W (in 25 MeV bins) was 1.4-1.9 GeV for the first two bins in the invariant momentum transfer Q^2, 0.5-0.8 (GeV/c)^2 and 0.8-1.1 (GeV/c)^2, and 1.4-2.1 GeV for the highest Q^2 bin, 1.1-1.5 (GeV/c)^2. Data were corrected for acceptance, reconstruction efficiency, radiative effects, and empty target counts [10]. In particular, a specifically developed Monte Carlo code was used to calculate the acceptance and efficiency. To this purpose, event distributions were generated in a realistic way and then processed through the GEANT-based code simulating the detector response. The same Monte Carlo event generator was used to perform extrapolations to kinematic regions where the acceptance vanishes. This type of corrections was typically only a few percent of the total cross section measured.

A particularly convenient set of kinematic variables for the analysis of resonance decay into $\Delta^{++}\pi^-$ (the dominant decay channel in the energy region considered here) is made up from the invariant mass of the $p\pi^+$ and the $\pi^+\pi^-$ pair, then the polar angles θ and ϕ of the π^- and finally the residual rotation freedom ψ of the $p\pi^+$ pair[13]. We derived experimental cross sections by binning and correcting the data in the full kinematic space defined by these variables, instead of applying a maximum likelihood procedure. The cross sections derived in our method can then be compared to any model calculation, knowledge of specific experimental features of the detector being unnecessary. We chose this approach as it is not sure *a priori* that models employed in the physics analysis (see below) are correctly describing the measured data distributions. On the other hand, a general partial-wave expansion is certainly very complicated and affected by strong ambiguities. We believe that our approach, being simple and direct, can provide a first interpretation of the data, revealing the most important features as the presence of isobars in the final state and the most prominent resonance excitations. In particular, missing state contributions with strong excitation in this channel can certainly be detected. Our analysis can provide a basis for future, more sophisticated searches based on likelihood functions and/or coupled channel calculations.

3 Physical analysis

Since existing theoretical models [14] are limited to W <1.6 GeV, we have employed a phenomenological calculation [15,16] for a first interpretation of the data. This model describes the reaction $\gamma_v p \to p\pi^+\pi^-$ in the kinematic range of interest as a sum of amplitudes for $\gamma_v p \to \Delta\pi \to p\pi^+\pi^-$ and $\gamma_v p \to \rho^0 p \to p\pi^+\pi^-$, according to the structures observed in the final state invariant mass distributions, while all other possible mechanisms are parameterized as phase space. A detailed treatment was developed for the non-resonant contributions to $\Delta\pi$, while for ρp production they were described through a diffractive ansatz. For the resonant part, a total of 12 states, classified with 3 and 4 stars [1], with sizeable $\Delta\pi$ and/or ρp decays, were included based on a Breit-Wigner ansatz. A few model parameters in non-resonant production were fitted to CLAS data at high W, where the non-resonant part creates a forward peaking in the angular distributions, and kept fixed in the subsequent analysis. The phase between resonant and non-resonant $\Delta\pi$ mechanisms was fitted to the CLAS data as well.

Resonance electromagnetic excitation was initially described through a Single Quark Transition Model (SQTM) fit[17], partial decay branches were taken from a previous analysis of hadronic data[18], and total widths were taken from PDG[1]. Even though our approach was that of a single channel analysis, we emphasize that, by using hadronic couplings from existing coupled channel analyses, we ensured that our resonance behavior was as compatible as possible with the information coming from other channels. This means that our resonance content was not completely derived from the CLAS data, with all inevitable ambiguities, but was constrained to the existing knowledge derived from the more sophisticated hadronic coupled channel techniques. Another important point regarding our analysis is that when calculating non-resonant terms for the $\Delta\pi$ channel, we applied an effective treatment of unitarity[15, 16], thereby taking into account the coupling to all other competing inelastic channels. Using this model approach, we first analysed the single-differential cross sections most sensitive to the dynamical content of our measurement[15, 16], i.e. $\frac{d\sigma}{dM_{p\pi^+}}$, $\frac{d\sigma}{dM_{\pi^+\pi^-}}$, and $\frac{d\sigma}{d\cos\theta_{\pi^-}}$, obtained by integrating over the other hadronic variables. These three 1-D distributions were then analysed or fitted simultaneously.

Starting from the above mentioned ingredients, we first produced a reference curve to be compared with the data (step (A) in text and figures). By reference curve, we mean

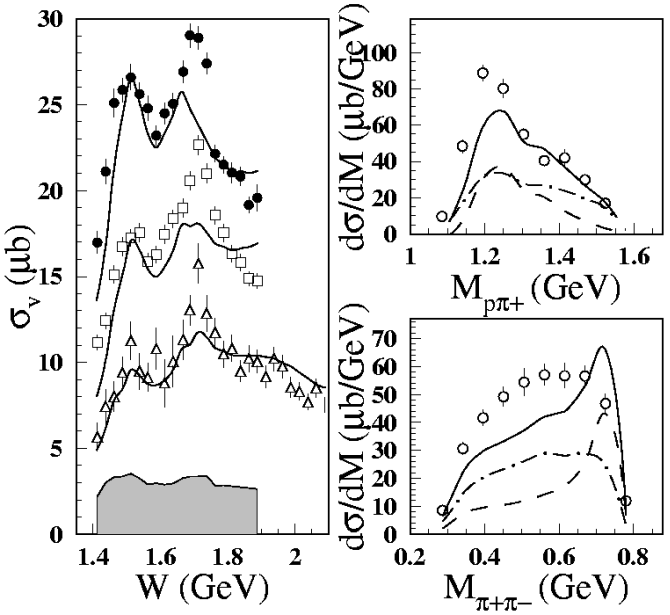

Fig. 1. *Left:* Total cross section for $\gamma_v p \to p\pi^+\pi^-$ as a function of W. Data from CLAS are shown at Q^2=0.5-0.8 (GeV/c)^2 (full points), Q^2=0.8-1.1 (GeV/c)^2 (open squares), and Q^2=1.1-1.5 (GeV/c)^2 (open triangles). Error bars are statistical only, while the bottom band shows the sytematic uncertainties for the lowest Q^2 bin. *Right:* $\frac{d\sigma_v}{dM_{p\pi^+}}$ (top) and $\frac{d\sigma_v}{dM_{\pi^+\pi^-}}$ (bottom) from CLAS at Q^2=0.8-1.1 (GeV/c)^2 and W=1.7-1.725 GeV (statistical error bars only). The curves represent our step (A) reference calculation: the dashed line includes all resonances, the dot-dashed line includes only the non-resonant part, and the solid line is the full calculation

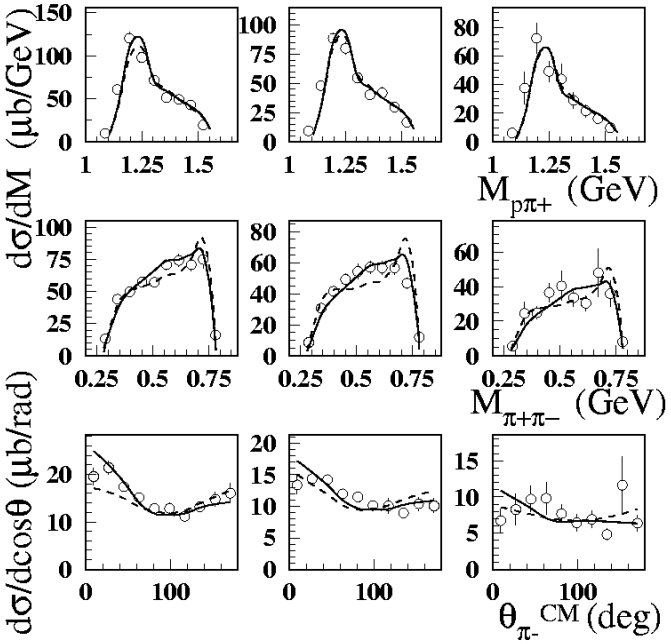

Fig. 2. $\frac{d\sigma_v}{dM_{p\pi^+}}$, $\frac{d\sigma_v}{dM_{\pi^+\pi^-}}$, and $\frac{d\sigma_v}{dcos\theta_{\pi^-}}$ from CLAS (from top to bottom) at W=1.7-1.725 GeV and for the three mentioned Q^2 intervals (left to right). The error bars include statistical errors only. Curves (see text) correspond to the fits (B2) (solid), and (B4) (dashed)

a set of total and differential cross sections obtained from our model without any parameter modification or fit. This reference calculation on one hand indicates how well we do in modeling non-resonant processes and how well the existing knowledge on all baryon resonances that contribute significantly to double pion electroproduction is reflected in the data. Any deviation of the data from this reference curve may therefore indicate either that our approach to non-resonant processes has basic problems, or that some resonance properties are not correctly accounted for in the existing database, or that some anomalous behavior is manifesting in the data, which in turn may signal the presence of new states or an unexpected microscopic structure of a known resonance. Results for step (A) are reported in Fig. 1. The total cross section strength for $W < 1.65$ GeV (except for the region close to threshold), and for $W >$ 1.8 GeV is well reproduced. Instead, a strong discrepancy is evident at W around 1.7 GeV. Moreover, at this energy the reference curve exhibits a lack of $\Delta\pi$ strength in the $p\pi^+$ invariant mass (Fig. 1, right top), and a strong peak in the $\pi^+\pi^-$ invariant mass (Fig. 1, right bottom), connected to sizeable ρ meson production. The latter was traced back to the 70-91% branching ratio of the $P_{13}(1720)$ into this channel[1,18,19].

Considering the resonance properties given by the PDG, and our limited knowledge on the Q^2 dependence of the photocouplings, the best ordinary candidates in providing the missing strength seen in the bump at 1.71 GeV are the $D_{13}(1700)$, the $P_{13}(1720)$, and the $P_{11}(1710)$ (the latter was not included in step (A)). Indeed, following the PDG, it seems that the bump at about W=1.7 GeV cannot be due to the $D_{15}(1675)$, $F_{15}(1680)$, or $D_{33}(1700)$ states; the first because its well known position cannot match the peak; the second because of its well known position and photocouplings [20]; the third due to its large width (∼300 MeV). Instead, there are no data available on the Q^2 dependence of $A_{1/2}$ or $A_{3/2}$ for the $D_{13}(1700)$, $P_{13}(1720)$, $P_{11}(1710)$ [20], and the hadronic couplings of the $D_{13}(1700)$ and the total width of the $P_{11}(1710)$ are poorly known. It is interesting to notice that, if no configuration mixing occurs, the $D_{13}(1700)$ cannot be excited in the SQTM from proton targets, while the SQTM prediction for the $P_{13}(1720)$ relies on ad hoc assumptions, since input data from states in the same multiplet are not sufficient [17].

Therefore we first performed three separate fits, (B1), (B2), and (B3), where the photo- and hadronic couplings of only one of those resonances at a time were widely varied, specifically the $D_{13}(1700)$ for (B1), the $P_{13}(1720)$ for (B2), and the $P_{11}(1710)$ for (B3). Our investigation at this stage was including the possibility of accounting for the 1.7 GeV structure via interference effects, although the peaking of such an interference pattern at the same W for all Q^2 bins would be rather surprising. Before proceeding with such fits, we performed slight variations of the initial curves from step (A), as allowed by the uncertainties in the knowledge of a number of states. All fit χ^2/ν values

were calculated from the 8 W bins between 1.64 and 1.81 GeV and from the 3 Q^2 bins (624 data points). The number of free parameters ranged from 11 to 32, depending on the fit, corresponding to ν=613 to 592 degrees of freedom. The best fit (χ^2/ν =3.4) was obtained in (B2) (Fig. 2). However, the resulting values for the branching fractions of the $P_{13}(1720)$ were significantly different from previous analyses reported in the literature and well outside the reported errors[1,18,19]. The corresponding fit of the total cross sections is reported as a dashed curve in Fig. 3. In a final multiresonance fit (B4), we varied only the electromagnetic excitation of all three candidate states, but no better solution was found (Fig. 2).

In the framework of our analysis, there is no way to assess the reliability of the previously determined hadronic parameters of the PDG $P_{13}(1720)$. The resonant content of the reaction $\pi N \to \pi\pi N$, which is used to obtain the hadronic parameters, may be different from that of reactions initiated by an electromagnetic probe. In particular, the $P_{13}(1720)$ state seen in $\pi N \to \pi\pi N$ may not be excited in electroproduction, while some other state that decouples from πN may be excited electromagnetically. We verified indeed that, if we introduced a new state as responsible for the observed bump, a good fit was obtained by a P_{I3} state (isospin could not be determined) with mass of about 1720 MeV, a width of about 90 MeV, about 40 % decay to $\Delta\pi$ and 17 % to ρp. The visual quality of the fit was very similar to the (B2) curves in Fig. 2. It is important to remark that such a good fit was achieved by using the published hadronic parameters for the ordinary $P_{13}(1720)$, while the electromagnetic amplitudes had to be suppressed with respect to the SQTM by about a factor 2 to avoid the mentioned unobserved ρ peak in the $\pi\pi$ invariant mass distribution. The quality of this fit was indistinguishable from the curves (B2) in Fig. 2. The quality of the fit of the total cross sections was also comparable to (B2), reported as a dashed curve in Fig. 3.

4 Using a Quark Model

To broaden the scope of our analysis and make cross section predictions using electromagnetic matrix elements from a fully theoretical picture, we introduced in our calculation the electromagnetic transition amplitudes from the Genova Hypercentral Quark Model (HQM) [21,8,22], including also the recently calculated longitudinal couplings, normally neglected in the resonance studies. The HQM incorporates the basic features of the SU(6) symmetry broken by an spin-isospin specific term. The potential used is based on the Coulomb attraction that dominates the short distances, together with a long distance linear confinement term. The form factors are derived from a one-body quark current operator and have been shown to describe quite well the existing data on the first excited resonances, specifically the $D_{13}(1520)$ and the $S_{11}(1535)$.

Using a quark model prediction instead of a fit, we do not change the basic assumptions about the degrees of freedom or the symmetries involved, but the electromagnetic amplitudes are predicted using a theoretical form for the current after fixing the model parameters from the spectrum properties alone. In fact, as mentioned above, in the SQTM most of the amplitudes are derived from experimental data, but in the case of the [70,1$^-$] multiplet the lack of experimental information forces to make ad hoc assumptions on the behavior of specific terms in the parameterization of the transition amplitudes, which makes the prediction affected both by the behavior of the data used in the fits, and by the assumptions made to supplement the missing experimental information. Therefore we can conclude that using a fully theoretical quark model prediction instead of a quark model fit really makes some difference in comparing to experimental data on the electromagnetic excitation of resonances.

In Fig. 3 we report the total cross sections from CLAS at the three 4-momentum transfers mentioned before, together with the calculated curves coming from the HQM. In one case (dot-dashed line) the curve was obtained by using directly all the HQM electromagnetic amplitudes for all the resonances considered. Then, the calculation was modified increasing the strength of the Roper resonance as indicated also by our first analysis based on the SQTM (solid line), and as also indicated by the lack of strength at low W in the HQM calculation. It is important to remark that we also included the prediction from the HQM about the longitudinal resonance couplings, often neglected in many analyses. Our resonance fit based on the SQTM is also shown for comparison (dashed line).

As clearly shown in Fig. 3, we still observe a considerable lack of strength in the region around 1.7 GeV, where the strong bump in the data is barely visible in the calculation. It seems therefore that two different analyses, one based on a general model-independent form for the transition matrix elements with parameters derived from existing data, the other based on a specific theoretical form for the quark transition current with no constraints from the data besides those necessary to reproduce the spectrum, are not able to explain the structure seen in the new CLAS data. To test once again the hypothesis that the observed peak may come from a new state, we took the parameters for the new resonance obtained in our previous fits and included the new state on top of the others calculated with the HQM amplitudes, with slight parameter adjustments. In Fig. 4, the result, plotted as the solid line, is compared to the HQM calculation containing only ordinary states and the modified Roper, plotted as the dashed line. It seems that the inclusion of the new state is compatible with the HQM resonance amplitudes, too.

At this point, it is natural to ask whether the differential cross sections are reproduced. In Fig. 5, I report such comparison between the CLAS data on top of the bump at 1.71 GeV and the HQM calculation with the addition of the new state: once again, the inclusion of the new state on top of the theoretical N* prediction provides a rather good match to the CLAS data.

From the two analyses performed, there emerges an indication that the electromagnetic excitation strength shown by the CLAS data is underestimated by single quark transition models, both phenomenological as well as fully theoretical. This may indicate different things: 1)

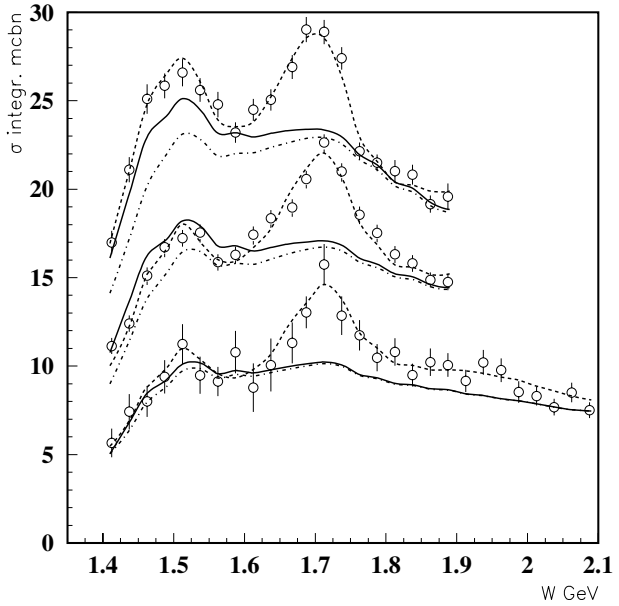

Fig. 3. Comparison of the CLAS data to a calculation based on resonant electromagnetic amplitudes from the HQM. The data are from CLAS at the three mentioned momentum transfers. The dot-dashed line is the calculation within the Genova-Moscow model using all resonance electromagnetic amplitudes (including longitudinal ones) from the HQM. The solid line is the calculation within the Genova-Moscow model using all resonance electromagnetic amplitudes (including longitudinal ones) from the HQM except for the Roper, which is taken from our previous fits. For comparison, we report as the dashed line our final fit starting from the SQTM amplitudes

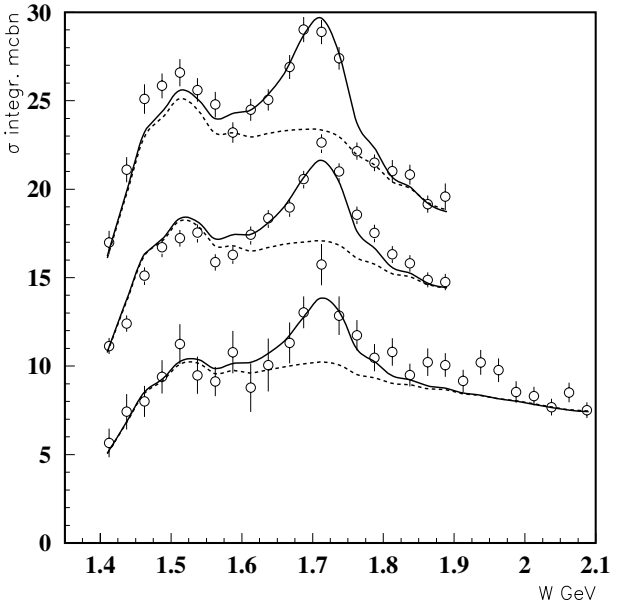

Fig. 4. Comparison of the CLAS data to a calculation based on resonant electromagnetic amplitudes from the HQM. The data are from CLAS at the three mentioned momentum transfers. The dashed line is the calculation within the Genova-Moscow model using all resonance electromagnetic amplitudes (including longitudinal ones) from the HQM except for the Roper, which is taken from our previous fits. The solid line is obtained by adding to the ordinary N* states calculated by the HQM the new state found in our previous fits

the single quark transition picture may be wrong, and we may be observing more complicated excitation mechanisms, with a redistribution of the strength; 2) additional degrees of freedom, like $q\bar{q}$ pairs, may modify the electromagnetic excitation, although their effect should disappear at higher Q^2, at variance with our observations; an admixture of exotic components cannot be excluded, either [23]; 3) the missing strength in the model analysis may be really due to the presence of one or more additional resonances, not observed before.

5 Conclusions

In conclusion, two pion production is one of the main subjects of investigation in Hall B at Jefferson Lab, as a key channel for extending our knowledge of light-quark baryons. The new high quality data from CLAS have shown the clear presence of resonance structures, not visible in the previous, technically limited experiments. In analysing the new data from CLAS, we adopted a phenomenological approach, based on the database of measured electromagnetic and hadronic resonance properties, and with effective unitarity constraints on the most relevant non-resonant mechanisms. Our analysis of the data has revealed that the prominent structure at 1.7 GeV seems difficult to explain when quark model fits or the-

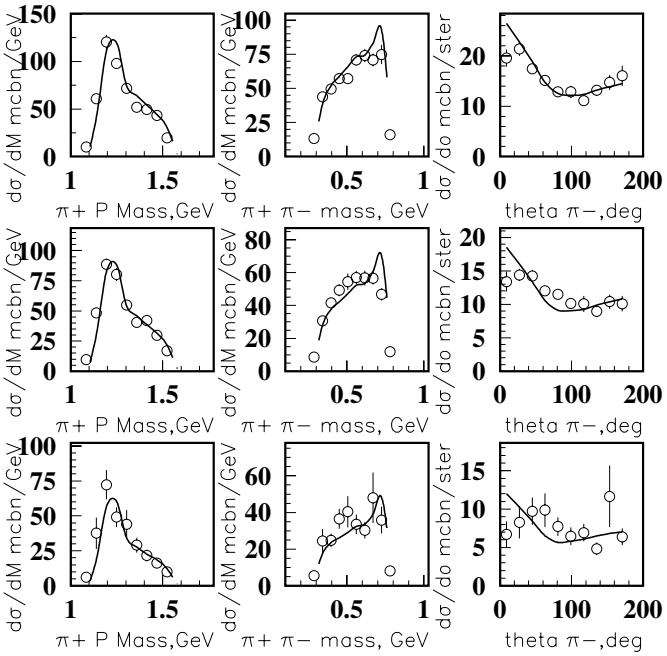

Fig. 5. $\frac{d\sigma_v}{dM_{p\pi^+}}$, $\frac{d\sigma_v}{dM_{\pi^+\pi^-}}$, and $\frac{d\sigma_v}{dcos\theta_{\pi^-}}$ from CLAS (left to right) at W=1.7-1.725 GeV and for the three mentioned Q^2 intervals (from top to bottom). The error bars include statistical errors only. The solid line is obtained by adding to the ordinary N* states calculated by the HQM the new state found in our previous fits

oretical predictions are used for the electromagnetic transition matrix elements. Moreover, the expected N* branching fractions to $\Delta\pi$ and ρp seem to be quite different from those inferred from the experimental mass distributions. A good data fit is indeed obtained by varying the properties of the ordinary $P_{13}(1720)$, but at the price of significantly changing the electromagnetic form factors with respect to the model expectations and at the additional price of attributing to this state branching fractions significantly different from the existing hadronic analyses. Both our analyses, based on quark model fits or fully theoretical amplitudes, alternatively indicated that the new CLAS cross sections are compatible with the presence of a new, unobserved state, although alternative scenarios involving multiquark transition, additional degrees of freedom, or exotic components cannot be ruled out.

References

1. K. Hagiwara et al.: Phys. Rev. D **66**, 010001 (2002)
2. R. Koniuk and N. Isgur: Phys. Rev. Lett. **44**, 845 (1980); Phys. Rev. D **21**, 1868 (1980)
3. R. Koniuk: Nucl. Phys., B **195**, 452 (1982)
4. S. Capstick and W. Roberts: Phys. Rev. D **49**, 4570 (1994)
5. F. Stancu and P Stassart: Phys. Rev. D **47**, 2140 (1993)
6. M. Kirchbach: Mod. Phys. Lett. A **12**, 3177 (1997)
7. M.M. Giannini: Rep. Prog. Phys. **54**, 453 (1991)
8. M. Aiello et al.: Phys. Lett. B **387**, 215 (1996)
9. M. Ripani: in Proceedings of the ICTP 3rd International Conference on Perspectives in Hadronic Physics, Trieste, Italy, 7–11 May 2001; Nucl. Phys. A **699**, 270 (2002)
10. M. Ripani et al.: hep-ex/0304034
11. B. Mecking et al.: Nucl. Inst. Meth. A **503**, 513 (2003); W. Brooks: Proc. of PANIC '99, Uppsala, Sweden, 10–16 June 1999, Nucl. Phys. A **663&664**, 29c (2000)
12. M. Ripani et al.: Phys. Rev. Lett. **91**, 022002 (2003)
13. Byckling and Kajantie: Particle kinematics, Wiley and Sons (1973)
14. J.C. Nacher and E. Oset: Nucl. Phys. A **674**, 205 (2000), and related work referenced therein
15. M. Ripani et al.: Nucl. Phys. A **672**, 220 (2000)
16. V. Mokeev et al.: Phys. of Atomic Nucl. **64**, 1292 (2001)
17. V.D. Burkert et al.: Phys. Rev. C **67**, 035204 (2003)
18. D.M. Manley and E.M. Salesky: Phys. Rev. D **45**, 4002 (1992)
19. T.P. Vrana et al.: Phys. Rept. **328**, 181 (2000)
20. V. Burkert: Nucl. Phys. A **684**, 16c (2001)
21. E. Santopinto: in these Proceedings
22. M. Aiello et al.: J. Phys. **G** 24, 753 (1998)
23. H. Walliser and V.B. Kopeliovich: hep-ph/0304058